nature neuroscience

Membrane potential correlates of sensory perception in mouse barrel cortex

Shankar Sachidhanandam, Varun Sreenivasan, Alexandros Kyriakatos, Yves Kremer & Carl C H Petersen

Neocortical activity can evoke sensory percepts, but the cellular mechanisms remain poorly understood. We trained mice to detect single brief whisker stimuli and report perceived stimuli by licking to obtain a reward. Pharmacological inactivation and optogenetic stimulation demonstrated a causal role for the primary somatosensory barrel cortex. Whole-cell recordings from barrel cortex neurons revealed membrane potential correlates of sensory perception. Sensory responses depended strongly on prestimulus cortical state, but both slow-wave and desynchronized cortical states were compatible with task performance. Whisker deflection evoked an early (<50 ms) reliable sensory response that was encoded through cell-specific reversal potentials. A secondary late (50–400 ms) depolarization was enhanced on hit trials compared to misses. Optogenetic inactivation revealed a causal role for late excitation. Our data reveal dynamic processing in the sensory cortex during task performance, with an early sensory response reliably encoding the stimulus and later secondary activity contributing to driving the subjective percept.

Sensory stimuli evoke action potential firing in modality-specific primary sensory neocortical regions that correlates with psychophysical measurements of sensory perception[1–4]. Direct stimulation of neocortical activity can evoke or bias sensory percepts that are related to the receptive field of the stimulated region[5–7]. Localized lesions in the neocortex and pharmacological or optogenetic blockade of neocortical action potential firing can cause pronounced and highly specific deficits in sensory perception[7–9]. Thus, there is substantial evidence to support the hypothesis that action potential firing in neocortical neurons generates sensory percepts. Action potentials in neocortical neurons are evoked by synaptic inputs depolarizing the membrane potential (V_m) beyond threshold. To obtain a causal and mechanistic understanding of sensory perception, it is therefore essential to understand the underlying V_m dynamics of neocortical neurons.

In vivo recordings investigating the neocortical V_m during sensory processing in awake animals have so far been limited to naive animals, which were not required to respond in any specific manner to perceived stimuli[10–13]. Such experiments have shown that V_m processing of stimuli in the primary sensory cortex of naive animals depends strongly on ongoing behavior and cortical state[10,14]. Extracellular recordings of neocortical activity in trained animals performing learned tasks have revealed profound modulation of the primary sensory cortex depending on the behavioral context, demonstrating strong top-down control of sensory processing[15,16]. However, the V_m dynamics of cortical states and sensory processing during task execution remain unknown. Here we developed a simple tactile whisker-dependent detection task in head-restrained mice and demonstrate that it depends on the primary somatosensory (S1) barrel cortex[17–19]. V_m recordings showed that a surprisingly large range of cortical states are compatible with task execution and revealed dynamic stimulus encoding with an early reliable sensory response that was invariant to behavioral outcome followed by a late secondary response, which both correlated with and contributed to the subjective sensory percept.

RESULTS

We trained mice to detect single deflections of the C2 whisker, reporting sensory perception through licking a reward spout to obtain water (**Fig. 1a**). Mice learned the task rapidly, reaching stable psychometric performance after a few daily training sessions (**Fig. 1b** and **Supplementary Fig. 1**). We delivered strong and reliable whisker deflection at random times without a cue by a 1-ms magnetic impulse acting on iron particles attached to the C2 whisker (**Supplementary Fig. 2**). Catch trials without stimuli were randomly interspersed, and a 2-s no-lick period was imposed before both the stimulus and catch trials.

S1 barrel cortex has a causal role in the detection task

The activity of neurons in the neocortex is thought to generate sensory percepts. We therefore tested for the involvement of the S1 whisker barrel cortex in our detection task. We mapped the S1 location of the C2 whisker barrel column using intrinsic signal optical imaging[17]. Injection of a voltage-gated sodium channel blocker (tetrodotoxin, TTX) into the C2 barrel column during behavioral sessions in well-trained mice produced a rapid and robust decrease in detection performance (**Fig. 1c**). Injection of TTX into S1 forepaw cortex had no effect on performance in the detection task, demonstrating the specific involvement of barrel cortex activity (**Fig. 1c**). Local field potential (LFP) recordings in the C2 barrel column indicated efficient blockade of the whisker-evoked cortical sensory response when TTX was injected into the C2 barrel column, and that the evoked response was little affected by TTX injection in S1 forepaw cortex (**Supplementary Fig. 3**). However, in addition to blocking local activity, TTX also blocks *en passant* fibers near the injection site. To inactivate

Laboratory of Sensory Processing, Brain Mind Institute, Faculty of Life Sciences, École Polytechnique Fédérale de Lausanne (EPFL), Lausanne, Switzerland. Correspondence should be addressed to C.C.H.P. (carl.petersen@epfl.ch).

Received 2 July; accepted 4 September; published online 6 October 2013; doi:10.1038/nn.3532

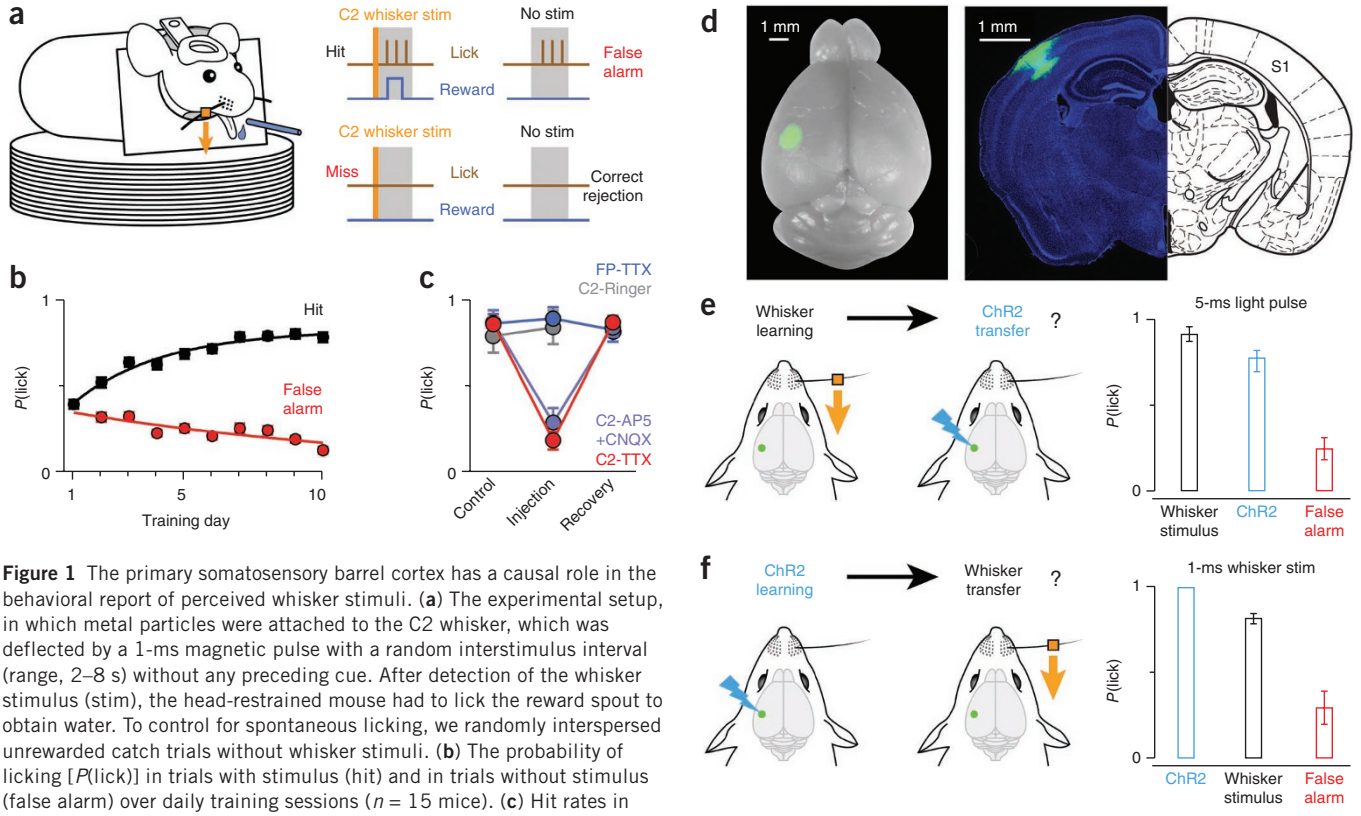

Figure 1 The primary somatosensory barrel cortex has a causal role in the behavioral report of perceived whisker stimuli. (**a**) The experimental setup, in which metal particles were attached to the C2 whisker, which was deflected by a 1-ms magnetic pulse with a random interstimulus interval (range, 2–8 s) without any preceding cue. After detection of the whisker stimulus (stim), the head-restrained mouse had to lick the reward spout to obtain water. To control for spontaneous licking, we randomly interspersed unrewarded catch trials without whisker stimuli. (**b**) The probability of licking [*P*(lick)] in trials with stimulus (hit) and in trials without stimulus (false alarm) over daily training sessions ($n = 15$ mice). (**c**) Hit rates in trained mice after injection of TTX or AP5 and CNQX into the C2 barrel column (C2-TTX, $n = 6$ mice; C2-AP5+CNQX, $n = 8$ mice). Also shown is the detection performance of mice after control injection of Ringer's solution into the C2 barrel column (C2-Ringer, $n = 4$ mice) or injection of TTX into the S1 forepaw representation (~1.5 mm away from the C2 barrel column; FP-TTX, $n = 4$ mice). (**d**) ChR2-YFP expression in excitatory neurons after injection of a Cre-dependent viral vector into the C2 barrel column of Emx1-Cre mice. Shown are images of the whole brain (left) with ChR2-YFP fluorescence (green) and a coronal section (right) stained with DAPI (blue) showing the middle of the injection site. (**e**) The experimental paradigm (left) and quantification of the results of the experiment (right) in which mice expressing ChR2 in S1 barrel cortex were first trained in the whisker detection task, and, afterwards, optogenetic stimulation of S1 barrel cortex was then interleaved with whisker stimulation and catch trials ($n = 6$ mice). (**f**) The experimental paradigm (left) and quantification of the results of the experiment (right) in which other mice were first trained to lick in response to 5 ms optogenetic stimulation of S1 barrel cortex. After reaching stable performance, whisker stimuli were interleaved with the optogenetic stimuli ($n = 3$ mice). The data in **b**, **c**, **e** and **f** are shown as the mean ± s.e.m.

with higher spatial specificity, we injected ionotropic glutamate receptor antagonists (6-cyano-7-nitroquinoxaline-2,3-dione (CNQX) and AP5 (D(−)-2-amino-5-phosphonovaleric acid) to block AMPA and NMDA receptors, respectively) into the C2 barrel column, in order to inhibit excitatory synaptic transmission. Injection of CNQX and AP5 reduced performance in our detection task, similar to the effect of TTX injection (**Fig. 1c**). Hence, action potential firing and glutamatergic synaptic transmission in S1 barrel cortex are necessary for whisker-stimulus detection as reported by goal-directed licking.

Neural activity in S1 barrel cortex might be causally related to sensory perception, driving downstream circuits that are involved in the sensorimotor transformation of a detected whisker stimulus into licking motor output. We expressed channelrhodopsin-2 (ChR2)[20] to test whether direct optogenetic stimulation of S1 barrel cortex could substitute for whisker deflection. We injected Cre-dependent ChR2 adeno-associated virus[21] into the C2 barrel column of Emx1-Cre mice to stimulate excitatory neurons (**Fig. 1d**). After training for the whisker detection task, optogenetic excitation of S1 barrel cortex readily substituted for whisker stimulation in all mice tested (whisker hit rate, 91 ± 4% (mean ± s.e.m.); S1 barrel cortex ChR2 hit rate, 75 ± 6%; false-alarm rate, 24 ± 7%; $n = 6$ mice) (**Fig. 1e** and **Supplementary Fig. 4**). We observed that mice displayed prominent whisker protraction after whisker stimulus in hit trials (**Supplementary Fig. 5**). As optogenetic stimulation of S1 evokes whisker movements[22], we investigated the impact of whisker movement on behavioral performance by transecting the facial nerve, which is the motor nerve that controls whisker movements. We found that facial nerve transection had no impact on performance, indicating that neither S1-driven retraction nor whisker protraction was necessary for our detection task (**Supplementary Fig. 5**). Mice trained to detect C2 whisker stimuli did not lick in response to optogenetic stimulation of the S1 forepaw cortex expressing ChR2 (whisker hit rate, 85 ± 5%; S1 forepaw ChR2 hit rate, 25 ± 8%; false-alarm rate, 8 ± 5%; $n = 3$ mice) (**Supplementary Fig. 4**). Direct optogenetic stimulation of S1 barrel cortex therefore readily and specifically substituted for peripheral whisker stimulation in trained mice, suggesting a causal role for action potential firing of barrel cortex neurons in our whisker detection task.

We next asked whether we could replace whisker stimulation by direct neocortical stimulation during the learning of the detection task. In a separate set of experiments, we trained naive mice to lick in response to single 5-ms optogenetic stimuli of excitatory neurons in S1 barrel cortex. In three out of four mice trained to lick in response to ChR2 stimulation of S1 barrel cortex, we found that single 1-ms C2 whisker deflections readily evoked licking (ChR2 hit rate, 100 ± 0%; whisker hit rate, 82 ± 3%; false-alarm rate, 29 ± 10%; $n = 3$ mice) (**Fig. 1f** and

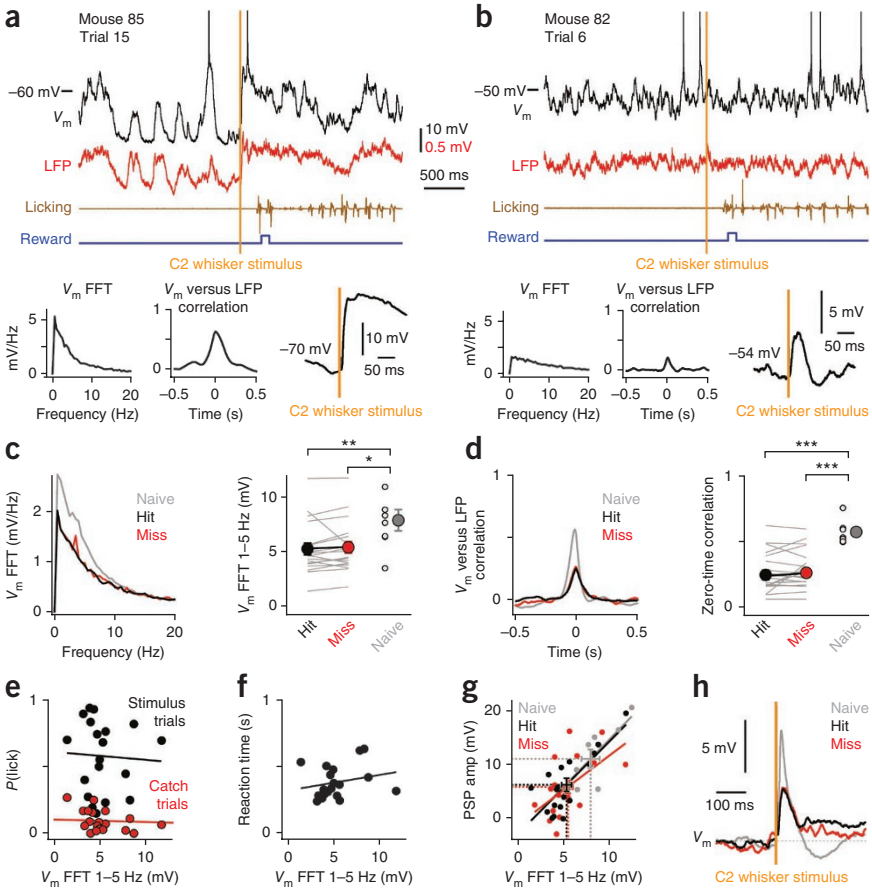

Figure 2 Diverse brain states are compatible with execution of the detection task. (**a**) Mouse 85 performed the detection task with a hit rate of 70% and a false-alarm rate of 5%. Prestimulus V_m indicated prominent slow fluctuations, which correlated with changes in LFP. FFT, fast Fourier transform. (**b**) Mouse 82 had a relatively desynchronized prestimulus brain state and performed with a hit rate of 69% and a false-alarm rate of 3%. (**c**) Grand average prestimulus V_m FFT amplitude spectrogram for hit and miss trials in trained mice and for naive mice (left) and the corresponding V_m 1–5 Hz FFT integral for each recording (right) (trained, $n = 19$ cells; naive, $n = 10$ cells; $P = 0.008$, hit compared to naive; $P = 0.01$, miss compared to naive; Wilcoxon-Mann-Whitney test). (**d**) Grand average prestimulus cross correlograms between V_m and LFP for hit and miss trials and naive mice (left) and the zero-time cross correlation for each recording (right) (trained, $n = 19$ cells; naive, $n = 9$ cells; $P = 0.00007$, hit compared to naive; $P = 0.0003$, miss compared to naive; Student's unpaired t test). (**e**) Hit rate and false alarm rate plotted with respect to prestimulus V_m 1–5 Hz FFT integral, quantified for each recording (linear correlation, stimulus trials $r = -0.053$, $P = 0.83$, t test; catch trials $r = -0.43$, $P = 0.06$, t test; $n = 19$ cells). (**f**) Reaction time plotted with respect to prestimulus V_m 1–5 Hz FFT (linear correlation, $r = 0.23$, $P = 0.34$, t test; $n = 19$ cells). (**g**) The PSP amplitude (amp) of the early sensory-evoked response quantified for each cell in both naive and trained mice. Crosses indicate mean values, and lines indicate the best fits for the hit, miss and naive data (linear correlation for hit trials: $r = 0.78$, $P = 0.00008$, t test, $n = 19$ cells; for miss trials: $r = 0.55$, $P = 0.015$, t test, $n = 19$ cells; for naive mice: $r = 0.82$, $P = 0.004$, t test, $n = 10$ cells). (**h**) The grand average membrane potential traces show that the early component of the sensory response was larger in naive mice, and the late depolarization was larger in trained mice, with a stronger late depolarization on hit trials compared to miss trials trained, $n = 19$ cells; naive, $n = 10$ cells). Circles (in **c**–**g**) and lines (in **c** and **d**) represent individual cells. Circles with error bars (in **c** and **d**) represent group averages and shown as mean ± s.e.m. $^*P < 0.05$, $^{**}P < 0.01$, $^{***}P < 0.001$. The action potential heights are truncated in the V_m traces. LFPs are shown inverted.

Supplementary Fig. 4). These experiments reveal that reward-based optogenetic training can be used to program behavior.

Diverse brain states are compatible with task performance

Having determined that the S1 whisker barrel cortex has a critical role in both the learning and execution of our detection task, we next investigated the underlying neural activity. We targeted whole-cell recordings to neurons located in layers 2 and 3 (2/3) of the C2 barrel column. Because cortical sensory processing depends strongly on brain state[10,14,23], we first characterized the patterns of spontaneous cortical activity in mice carrying out the detection task. To measure cortical network dynamics and synchrony, we correlated the V_m of individual neurons with the simultaneously recorded LFP during a 2-s prestimulus period in each trial. During task performance, different mice exhibited different brain states, ranging from slow, large-amplitude, highly correlated patterns of activity (**Fig. 2a**) to states that were dominated by more rapid asynchronous dynamics (**Fig. 2b**), with little variation within the same recording (**Supplementary Fig. 6**). We found no differences when comparing hit and miss trials in the frequency spectra of prestimulus V_m fluctuations (**Fig. 2c** and **Supplementary Fig. 7**) or in correlations of prestimulus V_m and LFP (**Fig. 2d**). Neither the probability of licking in response to whisker stimulation (**Fig. 2e**) nor the reaction time (**Fig. 2f**) showed dependence on cortical state. A wide range of brain states were therefore compatible with high performance in our detection task (**Fig. 2a–f** and **Supplementary Fig. 7**).

We found a strong influence of brain states on the sensory processing of whisker stimuli. Neurons recorded in mice with larger slow V_m fluctuations had larger-amplitude whisker-evoked postsynaptic potentials (PSPs) (**Fig. 2g**). The relationship was remarkably strong given that it was computed across cells in different mice. There was no difference when comparing hit and miss trials in the correlation of PSP amplitude with the amplitude of slow V_m fluctuations measured across different cells (**Fig. 2g**).

Comparison of trained and naive mice revealed marked similarities and differences. Naive mice (habituated to head restraint, as in previous studies[10,24], but not otherwise trained in the detection task) had significantly larger 1–5 Hz V_m fluctuations, and V_m was significantly more correlated with LFP in naive mice compared to trained mice (**Fig. 2c,d** and **Supplementary Fig. 7**). We observed a similar relationship between PSP amplitude and slow V_m fluctuations in trained and naive mice (**Fig. 2g**). The early depolarizing response was larger in naive mice than in trained mice (PSP amplitude quantified during the first 50 ms after whisker stimulus: naive mice, 11.1 ± 1.7 mV (mean ± s.e.m.), $n = 10$ cells; trained mice on hit trials, 6.3 ± 1.2 mV, $n = 19$ cells; Student's unpaired t test $P = 0.03$) (**Fig. 2h** and **Supplementary Fig. 8**).

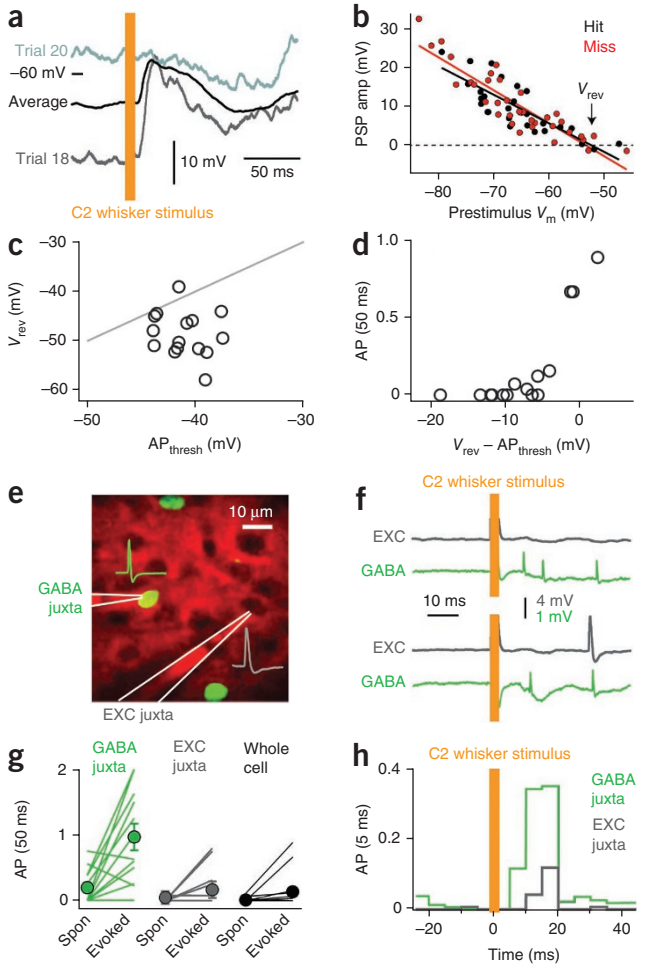

Figure 3 Reliable sparse coding of the sensory stimulus. (**a**) Whisker deflection transiently drove V_m toward a defined potential in two example hit trials and in the average response for the same recording. (**b**) The PSP amplitude of the early sensory response for the same cell plotted as a function of spontaneous prestimulus V_m across hit and miss trials. Whisker stimulus drives V_m to a cell-specific reversal potential (V_{rev}) (linear correlation for hit trials: $r = -0.83$, $P = 3 \times 10^{-8}$, t test, $n = 29$ trials; for miss trials: $r = -0.90$, $P = 9 \times 10^{-14}$, t test, $n = 36$ trials). (**c**) V_{rev} values for the hit trials with respect to the action potential threshold (AP_{thresh}; line of equality shown in gray). (**d**) The dependence of action potential firing during the early sensory response in hit trials on the difference between V_{rev} and the action potential threshold. (**e**) A two-photon image showing simultaneous juxtasomal (juxta) recording electrodes targeted to GFP-labeled GABAergic (GABA) neurons in GAD67-GFP mice (green) and to unlabeled excitatory (EXC) neurons visualized as shadows with Alexa-594 (red) in the extracellular space. (**f**) Two example hit trials showing simultaneous recordings of spikes in an excitatory neuron (gray) and in a GABAergic neuron (green). (**g**) Spontaneous prestimulus action potentials (Spon; quantified in the 50 ms before whisker stimulus) and whisker deflection–evoked action potentials (quantified in the 50 ms after whisker stimulus) during hit trials in GABAergic neurons compared to excitatory neurons ($n = 12$ juxtasomal recordings from GABAergic neurons; $n = 12$ juxtasomal recordings from excitatory neurons; $n = 19$ whole-cell recordings). (**h**) Grand average peristimulus time histogram of action potential firing in simultaneous juxtacellular recordings of excitatory and GABAergic neurons ($n = 12$ juxtasomal recordings from GABAergic neurons; $n = 12$ juxtasomal recordings from excitatory neurons). Circles (in **b**) represent individual trials. Circles (in **c** and **d**) and lines (in **g**) represent individual cells. Circles with error bars (in **g**) represent group averages and are shown as the mean ± s.e.m.

Spike rates during the early sensory response were also higher in naive mice (action potential rate quantified from 0 to 50 ms after whisker stimulus: hit, 3.1 ± 1.0 Hz, $n = 31$ cells, including 19 whole-cell recordings and 12 juxtasomal recordings; naive, 5.7 ± 1.1 Hz, $n = 17$ cells, including 10 whole-cell recordings and 7 juxtasomal recordings; Wilcoxon-Mann-Whitney test $P = 0.002$) (**Supplementary Fig. 8**)[25]. As naive mice had larger 1–5 Hz V_m fluctuations than trained mice on average (**Fig. 2c**), their larger-amplitude early sensory responses likely resulted from brain-state differences (**Fig. 2g**)[10,23]. The relatively desynchronized brain state of trained mice on average might be driven by increased thalamic action potential firing[26], as well as neuromodulatory input[27]. As discussed further below, trained mice exhibited an additional late depolarization, which was largest on hit trials and strongly reduced in naive mice (**Fig. 2h** and **Supplementary Fig. 8**).

A reliable early response invariant to behavioral outcome

A large amount of the variability in PSP response amplitude comparing recordings in different mice can be accounted for by differences in brain state (**Fig. 2**). We next examined trial-by-trial variability of the early sensory response within individual recordings. The PSP amplitude varied strongly across trials depending linearly on the spontaneous prestimulus V_m with a cell-specific reversal potential (V_{rev}) (**Fig. 3a**,**b**). There was no difference in prestimulus V_m, prestimulus action potential rates, PSP amplitudes, V_{rev} or evoked action potential firing within 50 ms when comparing hit and miss trials (**Supplementary Fig. 9**). For most cells, V_{rev} was hyperpolarized relative to the action potential threshold (V_{rev} hit, −48.5 ± 1.2 mV (mean ± s.e.m.); action potential threshold, −41.1 ± 0.6 mV; $n = 15$ cells) (**Fig. 3c**), and the difference between V_{rev} and the action potential threshold predicted evoked firing (**Fig. 3d**). Our *in vivo* whole-cell recordings therefore suggest that the early sensory response can be described as a state vector of cell-specific reversal potentials toward which the neuronal network is driven by whisker deflection[28].

Local GABAergic inhibitory neurons could contribute to driving a hyperpolarized V_{rev}. We therefore performed simultaneous juxtasomal recordings of nearby excitatory and inhibitory neurons in the C2 barrel column of GAD67-GFP mice[28,29] during task performance (**Fig. 3e–h**). Our recordings revealed that GABAergic neurons fired more action potentials than excitatory neurons (quantified during the first 50 ms after whisker stimulus: excitatory neurons fired 0.18 ± 0.09 (mean ± s.e.m.) action potentials per trial, $n = 12$ cells; GABAergic neurons fired 0.96 ± 0.20 action potentials per trial, $n = 12$ cells; Student's unpaired t test $P = 0.002$) (**Fig. 3g**). GABAergic neurons also fired earlier than the simultaneously recorded excitatory neurons (**Fig. 3h**). The generally hyperpolarized nature of the reversal potential of the early sensory-evoked response may therefore be driven by action potential firing of nearby GABAergic neurons, which provide strong inhibition onto excitatory layer 2/3 mouse barrel cortex neurons[30].

The distribution of evoked action potential firing across juxtasomal recordings from excitatory neurons agreed closely with whole-cell recordings indicating the relatively reliable firing of ~15% of layer 2/3 excitatory neurons within the C2 barrel column (**Fig. 3g**). In juxtasomal recordings, 2 out of the 12 excitatory cells fired robustly (0.77 spikes per stimulus), whereas the remaining 10 excitatory cells fired little (0.06 spikes per stimulus) within 50 ms of whisker stimulus. For whole-cell recordings, 3 out of the 19 cells fired robustly (0.70 spikes per stimulus), whereas the remaining 16 cells responded poorly (0.02 spikes per stimulus).

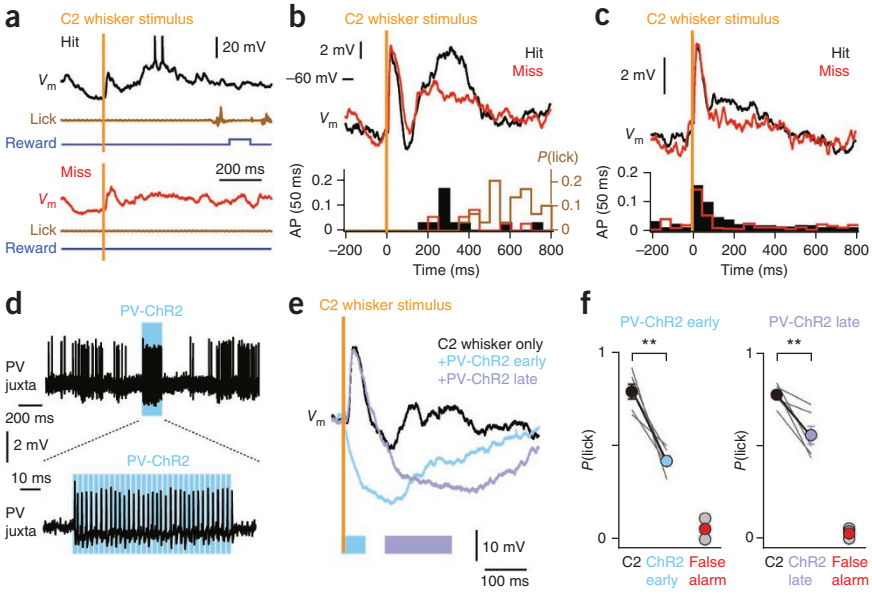

Figure 4 Late depolarization and action potential firing correlate with and causally contribute to behavioral report of sensory perception. (**a**) Example hit and miss trials during whole-cell V_m recording (the action potential height is truncated). (**b**) For the same recording, the averaged V_m across all hit and miss trials from the same cell ($n = 29$ hit trials; $n = 36$ miss trials). (**c**) Grand average V_m ($n = 19$ whole-cell recordings) and action potential firing ($n = 31$ cells, comprising 12 juxtasomal and 19 whole-cell recordings) in excitatory neurons. (**d**) Juxtasomal recording of a PV-expressing neuron, targeted through two-photon microscopy, during application of a 200-Hz blue light pulse train. (**e**) Optogenetic stimulation of ChR2-expressing PV-neurons (PV-ChR2) rapidly hyperpolarized nearby excitatory neurons by ~10 mV, which lasted ~200 ms. Early application of blue light (immediately before the whisker stimulus) completely blocked the sensory response. Late blue light stimulation (starting 100 ms after the whisker stimulus) left the early sensory response intact but specifically hyperpolarized excitatory neurons during the late secondary response. Traces show V_m averaged across hit and miss trials for each condition. (**f**) Detection performance after either early or late optogenetic inactivation of S1 barrel cortex ($n = 6$ mice). Circles and lines (in **f**) represent individual cells, circles with error bars represent group averages. The data in **f** are shown as the mean ± s.e.m. $^{**}P < 0.01$, Student's paired t test.

Late excitation contributes causally to perceptual report

Our V_m recordings revealed that mice trained in the detection task exhibited a late depolarization in response to whisker stimulation, which was strongly reduced in naive mice (**Fig. 2h**). In trained mice, the late depolarization was significantly larger on hit trials compared to miss trials (mean V_m quantified from 50 to 400 ms after whisker stimulus: hit, −57.5 ± 1.0 mV; miss, −59.1 ± 1.2 mV; Student's paired t test $P = 0.03$; $n = 19$ cells) (**Fig. 4a–c** and **Supplementary Fig. 9**). Significantly increased action potential firing accompanied the late depolarization on hit trials (action potential rate quantified from 50 to 400 ms after whisker stimulus: hit, 0.70 ± 0.23 Hz; miss, 0.35 ± 0.13 Hz; Wilcoxon signed-rank paired test $P = 0.04$; $n = 31$ cells, including 19 whole-cell recordings and 12 juxtasomal recordings) (**Fig. 4c** and **Supplementary Fig. 9**). Furthermore, we also observed enhanced late depolarization in hit trials compared to miss trials in mice with facial nerve transection, suggesting that the late depolarization is generated by internal brain circuits rather than sensory reafference coming from associated whisker movements (**Supplementary Fig. 10**).

Whereas the early component of the sensory response reliably represents the sensory stimulus, the late component correlates with the subjective perceptual report. Notably, the late depolarization and late spiking preceded licking, by hundreds of milliseconds in some cases (**Fig. 4a**), thus potentially having a causal role in perceptual report. To test this hypothesis, we expressed ChR2 in parvalbumin (PV)-expressing GABAergic neurons (**Fig. 4d** and **Supplementary Fig. 11**)[21,31], which provide powerful inhibition to nearby excitatory barrel cortex neurons[30], enabling rapid optogenetic inhibition of the local neocortical microcircuit. We verified the efficacy of this method by applying a blue light pulse train beginning immediately before the whisker stimulus, which completely blocked the cortical sensory response evoked by the C2 whisker stimulus (**Fig. 4e**). This early optogenetic inhibition protocol profoundly suppressed detection performance (control hit rate, 79 ± 4%; early PV-ChR2 hit rate, 42 ± 3%; false-alarm rate, 6 ± 1%; $n = 6$ mice; Student's paired t test $P = 0.002$ for control compared to early PV-ChR2 hit rate) (**Fig. 4f**). This result confirms the key role of S1 barrel cortex in our whisker detection task, as we found in our pharmacological inactivation experiments (**Fig. 1c**). We next optogenetically inhibited S1 barrel cortex during the secondary late response period by applying blue light pulse trains starting 100 ms after whisker deflection. The early sensory response recorded in excitatory neurons was unaffected, but blue light caused a rapid ~10 mV hyperpolarization that lasted hundreds of milliseconds during the time when the late secondary response would normally be observed in hit trials (**Fig. 4e**). This late inactivation of S1 cortex also reduced detection performance (control hit rate, 78 ± 2%; late PV-ChR2 hit rate, 56 ± 5%; false-alarm rate, 3 ± 1%; $n = 6$ mice; Student's paired t test $P = 0.007$ for control compared to late PV-ChR2 hit rate) (**Fig. 4f**). The effects were specific to inactivation of the barrel cortex, as we observed no deficit in behavior in control experiments in which ChR2 was expressed and activated in PV-expressing neurons of the forepaw S1 during the whisker detection task (**Supplementary Fig. 11**). Therefore, the late depolarization and late spiking of excitatory barrel cortex neurons not only correlate with the behavioral report of perceived stimuli but also have a causal role in driving the downstream circuits that are responsible for initiating licking.

DISCUSSION

A key goal for neuroscience is to obtain a causal and mechanistic explanation for sensory perception at the level of synaptic interactions between individual neurons within specific neural circuits of the mammalian brain. Because this is a difficult challenge, it may be helpful to examine very simple forms of sensory perception, which might then be investigated in detail. Here we trained head-restrained mice to detect a 1-ms deflection of the C2 whisker delivered at a random time and report perceived stimuli by licking a spout to obtain a water reward. We demonstrated a critical role for neuronal activity in S1 barrel cortex (**Fig. 1**) and subsequently measured the V_m dynamics of neocortical layer 2/3 neurons in the C2 barrel column during task performance. Because brain states are influenced profoundly by behavior and, conversely, brain states strongly affect sensory processing, we first investigated the prestimulus cortical state (**Fig. 2**). We next investigated the evoked response and found that

it consisted of two components: an early reliable sensory response that did not differ when comparing hit and miss trials (**Fig. 3**) and a later secondary depolarization that was enhanced in hit trials and causally contributed to driving the behavioral report of the subjective percept (**Fig. 4**).

We established the necessity of S1 barrel cortex activity in the execution of the detection task by several different manipulations. Local injections targeted to the C2 barrel column of either TTX to block action potentials or CNQX and AP5 to block ionotropic glutamatergic synaptic transmission prevented task execution (**Fig. 1c**). However, pharmacological inactivation lasting many minutes might induce profound changes in brain states and neuronal activity in other brain areas that are directly or indirectly connected to S1 barrel cortex. An essential further experiment was therefore to inactivate S1 barrel cortex optogenetically with high temporal precision, which revealed the specific requirement for S1 barrel cortex neural activity during the sensory response on the millisecond timescale (**Fig. 4d–f**). Notably, identical manipulations applied to S1 forepaw cortex (**Fig. 1c** and **Supplementary Fig. 11**) did not affect behavior, pointing to the specific involvement of the barrel cortex. Our results contrast with lesion experiments that suggested that only complex whisker behaviors require S1 barrel cortex[8] but are in good agreement with more recent pharmacological[9] and optogenetic[7] inactivation experiments.

We were also able to readily substitute the peripheral sensory whisker deflection during task performance by an optogenetic stimulus delivered to excitatory neurons in S1 barrel cortex (**Fig. 1e**). These results are in good agreement with previous experiments in which peripheral stimuli were successfully replaced by direct cortical stimulation[5–7]. In addition, we found that we could train mice to detect S1 optogenetic stimulation and that after this optogenetic programming of behavior, mice would also lick in response to whisker stimulation (**Fig. 1f**). Here the optogenetic S1 stimulus drove the learning of the task. These data might suggest that reward-based learning of the sensorimotor transformation that associates a sensory stimulus with goal-directed motor output might occur in brain areas downstream of S1, perhaps involving corticostriatal pathways[32].

The optogenetic inactivation and substitution experiments together provide strong evidence that S1 barrel cortex forms an essential node in the neural circuit underlying our detection task. We therefore investigated the patterns of neuronal activity in S1 barrel cortex during task execution. We found that a wide range of cortical states defined through simultaneous whole-cell V_m and LFP recordings were compatible with high performance in our detection task (**Fig. 2**). Mice in cortical states with prominent slow V_m fluctuations that were highly synchronized with LFP fluctuations could execute the detection task with equally high success rates (**Fig. 2e**) and equivalent reaction times (**Fig. 2f**) compared to mice exhibiting desynchronized cortical states. This is surprising given that slow-wave cortical states have previously been associated with immobile wakefulness and sleep[10,11,24,26,28,29,33,34]. In future experiments, it will be important to examine whether differences in brain states affect the performance of more complex whisker-dependent tasks.

Cortical state varied little across trials within individual recordings but varied strongly across different mice. Differences in cortical state of different mice strongly affected the amplitude of the early sensory response, providing an explanation for a large part of the variability observed in the response amplitude in different recordings (**Fig. 2g**). Neurons recorded in mice with large-amplitude spontaneous slow V_m fluctuations also had large-amplitude sensory-evoked responses. Conversely, neurons recorded in mice with desynchronized cortical states had smaller-amplitude sensory responses. These data are in good agreement with previous measurements that studied the impact of cortical states on sensory processing in naive mice[10,14]. One explanation for the unexpected presence of brain states with large slow V_m fluctuations in mice performing the detection task is that the large sensory responses evoked from this brain state could be sufficiently strong to drive downstream neural circuits. Relaxed brain states might therefore be a useful adaptive behavioral strategy, particularly in a detection task without a cue, allowing for the robust detection of whisker stimuli occurring at random timing.

We found that the early short-latency response occurring within 50 ms of whisker deflection did not differ when comparing hit and miss trials in the same recording (**Fig. 2g**,**h**). Rather, the sensory response was reliably encoded in the form of a reversal potential with respect to variation in prestimulus V_m that was invariant to behavioral outcome (**Fig. 3b**). The reversal potentials were hyperpolarized in general with respect to the action potential threshold, thus evoking only sparse firing of layer 2/3 excitatory neurons, which is consistent with previous investigations of barrel cortex function in awake rodents[3,4,10,24,28,35–37]. The hyperpolarized reversal potentials of the early sensory response were likely driven by near-simultaneous arrival of excitatory and inhibitory synaptic conductances driven by feedforward thalamocortical and intracortical circuits[38]. In future experiments, it will be important to determine whether the small fraction of cells reliably firing action potentials is sufficient to drive perception and whether these cells belong to specific classes of excitatory projection neurons[39]. It will also be important to determine the contribution of various subtypes of GABAergic neurons[31] in driving the generally hyperpolarized reversal potential of the early sensory response during task performance.

Late excitation occurring 50–400 ms after whisker stimulation was prominent in trained mice but was absent in naive mice under our experimental conditions (**Fig. 2h**). Furthermore, late depolarization and action potential firing were enhanced in hit trials compared to misses (**Fig. 4a–c**). Notably, optogenetic inhibition of S1 barrel cortex during the late response period revealed that late excitation also causally participated in driving behavioral report (**Fig. 4d–f**). Late activity in S1 barrel cortex therefore participates in the conversion of the sensory signal (a 1-ms deflection of the C2 whisker) into a learned goal-directed motor output (licking the reward spout). It is important to note that in our detection task, we used strong whisker stimuli, and failure to lick therefore probably reflects deficiency in sensorimotor processing rather than stimulus variability. Differences in neuronal activity when comparing hit and miss trials might therefore result largely from top-down attentional, motivational and cognitive influences on the primary sensory cortex[15,16]. In our detection task, we found that late excitation correlated with and contributed to generating the subjective sensory percept. The mechanisms driving the late depolarization remain to be investigated. One attractive possibility is that the whisker deflection in trained mice generates a prediction of reward availability, which could be encoded through a phasic dopamine[40] or acetylcholine[41] signal. Such a neuromodulatory reward prediction signal could act on a variety of brain targets including (i) directly on excitatory neocortical neurons, (ii) indirectly through disinhibition in local neocortical microcircuits[42] or (iii) indirectly through brain areas connected to S1 barrel cortex. There are many brain areas that provide synaptic input to S1 barrel cortex, and the late depolarization on hit trials could result from enhanced activity in any of these areas. Of particular interest is the possible involvement of feedback inputs to S1 barrel cortex from reciprocally connected cortical areas, such as the motor cortex[14,22,43,44].

Internal motor commands from the motor cortex could provide a top-down source for the late response, perhaps through slow dendritic events[45–47] and disinhibition[11,48]. In future studies of this detection task, it will be important to study the role of specific subtypes of excitatory[39] and inhibitory neurons[31] in different cortical layers of S1 barrel cortex and uncover the neural circuits downstream of S1 (ref. 49) in the sensorimotor transformation from whisker stimulus to goal-directed licking. Whether late depolarization accompanies perceived stimuli of other sensory modalities and in other species remains to be determined. Interestingly, electroencephalography measurements from humans have suggested that late potentials are a hallmark of conscious perception[50], raising the possibility that our results may be of general importance.

METHODS

Methods and any associated references are available in the online version of the paper.

Note: Any Supplementary Information and Source Data files are available in the online version of the paper.

ACKNOWLEDGMENTS

This work was funded by grants from the Swiss National Science Foundation (31003A-116027 and 310030-146252), a joint grant between the Swiss National Science Foundation and the Deutsche Forschungsgemeinschaft (BaCoFun 310030E-147486), the Human Frontier Science Program (RGP0041/2009), SystemsX.ch (Neurochoice), the National Competence Centre for Research (Synapsy) and the European Research Council (ERC-2011-AdG-293660 Sensorimotor).

AUTHOR CONTRIBUTIONS

S.S. designed and set up the behavioral paradigm, carried out all of the electrophysiological recordings and optogenetic inhibition experiments and analyzed the data. V.S. and A.K. carried out the optogenetic substitution and optogenetic learning experiments and analyzed the data. Y.K. and S.S. built the two-photon microscope. C.C.H.P. contributed to the design of experiments and supervised the project. C.C.H.P. and S.S. wrote the manuscript. All of the authors commented on the manuscript.

COMPETING FINANCIAL INTERESTS

The authors declare no competing financial interests.

1. Parker, A.J. & Newsome, W.T. Sense and the single neuron: probing the physiology of perception. *Annu. Rev. Neurosci.* **21**, 227–277 (1998).
2. Luna, R., Hernández, A., Brody, C.D. & Romo, R. Neural codes for perceptual discrimination in primary somatosensory cortex. *Nat. Neurosci.* **8**, 1210–1219 (2005).
3. Stüttgen, M.C. & Schwarz, C. Psychophysical and neurometric detection performance under stimulus uncertainty. *Nat. Neurosci.* **11**, 1091–1099 (2008).
4. O'Connor, D.H., Peron, S.P., Huber, D. & Svoboda, K. Neural activity in barrel cortex underlying vibrissa-based object localization in mice. *Neuron* **67**, 1048–1061 (2010).
5. Salzman, C.D., Britten, K.H. & Newsome, W.T. Cortical microstimulation influences perceptual judgements of motion direction. *Nature* **346**, 174–177 (1990).
6. Romo, R., Hernández, A., Zainos, A. & Salinas, E. Somatosensory discrimination based on cortical microstimulation. *Nature* **392**, 387–390 (1998).
7. O'Connor, D.H. *et al.* Neural coding during active somatosensation revealed using illusory touch. *Nat. Neurosci.* **16**, 958–965 (2013).
8. Hutson, K.A. & Masterton, R.B. The sensory contribution of a single vibrissa's cortical barrel. *J. Neurophysiol.* **56**, 1196–1223 (1986).
9. Miyashita, T. & Feldman, D.E. Behavioral detection of passive whisker stimuli requires somatosensory cortex. *Cereb. Cortex* **23**, 1655–1662 (2013).
10. Crochet, S. & Petersen, C.C.H. Correlating whisker behavior with membrane potential in barrel cortex of awake mice. *Nat. Neurosci.* **9**, 608–610 (2006).
11. Gentet, L.J. *et al.* Unique functional properties of somatostatin-expressing GABAergic neurons in mouse barrel cortex. *Nat. Neurosci.* **15**, 607–612 (2012).
12. Haider, B., Häusser, M. & Carandini, M. Inhibition dominates sensory responses in the awake cortex. *Nature* **493**, 97–100 (2013).
13. Polack, P.O., Friedman, J. & Golshani, P. Cellular mechanisms of brain state–dependent gain modulation in visual cortex. *Nat. Neurosci.* **16**, 1331–1339 (2013).
14. Ferezou, I. *et al.* Spatiotemporal dynamics of cortical sensorimotor integration in behaving mice. *Neuron* **56**, 907–923 (2007).
15. Nienborg, H., Cohen, M.R. & Cumming, B.G. Decision-related activity in sensory neurons: correlations among neurons and with behavior. *Annu. Rev. Neurosci.* **35**, 463–483 (2012).
16. Gilbert, C.D. & Li, W. Top-down influences on visual processing. *Nat. Rev. Neurosci.* **14**, 350–363 (2013).
17. Petersen, C.C.H. The functional organization of the barrel cortex. *Neuron* **56**, 339–355 (2007).
18. Diamond, M.E., von Heimendahl, M., Knutsen, P.M., Kleinfeld, D. & Ahissar, E. 'Where' and 'what' in the whisker sensorimotor system. *Nat. Rev. Neurosci.* **9**, 601–612 (2008).
19. Feldmeyer, D. *et al.* Barrel cortex function. *Prog. Neurobiol.* **103**, 3–27 (2013).
20. Boyden, E.S., Zhang, F., Bamberg, E., Nagel, G. & Deisseroth, K. Millisecond-timescale, genetically targeted optical control of neural activity. *Nat. Neurosci.* **8**, 1263–1268 (2005).
21. Cardin, J.A. *et al.* Driving fast-spiking cells induces gamma rhythm and controls sensory responses. *Nature* **459**, 663–667 (2009).
22. Matyas, F. *et al.* Motor control by sensory cortex. *Science* **330**, 1240–1243 (2010).
23. Otazu, G.H., Tai, L.H., Yang, Y. & Zador, A.M. Engaging in an auditory task suppresses responses in auditory cortex. *Nat. Neurosci.* **12**, 646–654 (2009).
24. Poulet, J.F.A. & Petersen, C.C.H. Internal brain state regulates membrane potential synchrony in barrel cortex of behaving mice. *Nature* **454**, 881–885 (2008).
25. Gdalyahu, A. *et al.* Associative fear learning enhances sparse network coding in primary sensory cortex. *Neuron* **75**, 121–132 (2012).
26. Poulet, J.F.A., Fernandez, L.M., Crochet, S. & Petersen, C.C.H. Thalamic control of cortical states. *Nat. Neurosci.* **15**, 370–372 (2012).
27. Lee, S.H. & Dan, Y. Neuromodulation of brain states. *Neuron* **76**, 209–222 (2012).
28. Crochet, S., Poulet, J.F.A., Kremer, Y. & Petersen, C.C.H. Synaptic mechanisms underlying sparse coding of active touch. *Neuron* **69**, 1160–1175 (2011).
29. Gentet, L.J., Avermann, M., Matyas, F., Staiger, J.F. & Petersen, C.C.H. Membrane potential dynamics of GABAergic neurons in the barrel cortex of behaving mice. *Neuron* **65**, 422–435 (2010).
30. Avermann, M., Tomm, C., Mateo, C., Gerstner, W. & Petersen, C.C.H. Microcircuits of excitatory and inhibitory neurons in layer 2/3 of mouse barrel cortex. *J. Neurophysiol.* **107**, 3116–3134 (2012).
31. Lee, S.H. *et al.* Activation of specific interneurons improves V1 feature selectivity and visual perception. *Nature* **488**, 379–383 (2012).
32. Znamenskiy, P. & Zador, A.M. Corticostriatal neurons in auditory cortex drive decisions during auditory discrimination. *Nature* **497**, 482–485 (2013).
33. Timofeev, I., Grenier, F. & Steriade, M. Disfacilitation and active inhibition in the neocortex during the natural sleep-wake cycle: an intracellular study. *Proc. Natl. Acad. Sci. USA* **98**, 1924–1929 (2001).
34. Okun, M., Naim, A. & Lampl, I. The subthreshold relation between cortical local field potential and neuronal firing unveiled by intracellular recordings in awake rats. *J. Neurosci.* **30**, 4440–4448 (2010).
35. Huber, D. *et al.* Sparse optical microstimulation in barrel cortex drives learned behaviour in freely moving mice. *Nature* **451**, 61–64 (2008).
36. Houweling, A.R. & Brecht, M. Behavioural report of single neuron stimulation in somatosensory cortex. *Nature* **451**, 65–68 (2008).
37. de Kock, C.P. & Sakmann, B. Spiking in primary somatosensory cortex during natural whisking in awake head-restrained rats is cell-type specific. *Proc. Natl. Acad. Sci. USA* **106**, 16446–16450 (2009).
38. Petersen, C.C.H. & Crochet, S. Synaptic computation and sensory processing in neocortical layer 2/3. *Neuron* **78**, 28–48 (2013).
39. Chen, J.L., Carta, S., Soldado-Magraner, J., Schneider, B.L. & Helmchen, F. Behaviour-dependent recruitment of long-range projection neurons in somatosensory cortex. *Nature* **499**, 336–340 (2013).
40. Schultz, W. Getting formal with dopamine and reward. *Neuron* **36**, 241–263 (2002).
41. Chubykin, A.A., Roach, E.B., Bear, M.F. & Shuler, M.G. A cholinergic mechanism for reward timing within primary visual cortex. *Neuron* **77**, 723–735 (2013).
42. Letzkus, J.J. *et al.* A disinhibitory microcircuit for associative fear learning in the auditory cortex. *Nature* **480**, 331–335 (2011).
43. Mao, T. *et al.* Long-range neuronal circuits underlying the interaction between sensory and motor cortex. *Neuron* **72**, 111–123 (2011).
44. Huber, D. *et al.* Multiple dynamic representations in the motor cortex during sensorimotor learning. *Nature* **484**, 473–478 (2012).
45. Larkum, M.E., Nevian, T., Sandler, M., Polsky, A. & Schiller, J. Synaptic integration in tuft dendrites of layer 5 pyramidal neurons: a new unifying principle. *Science* **325**, 756–760 (2009).
46. Branco, T. & Häusser, M. The single dendritic branch as a fundamental functional unit in the nervous system. *Curr. Opin. Neurobiol.* **20**, 494–502 (2010).
47. Xu, N.L. *et al.* Nonlinear dendritic integration of sensory and motor input during an active sensing task. *Nature* **492**, 247–251 (2012).
48. Lee, S., Kruglikov, I., Huang, Z.J., Fishell, G. & Rudy, B. A disinhibitory circuit mediates motor integration in the somatosensory cortex. *Nat. Neurosci.* doi:10.1038/nn.3544 (6 October 2013).
49. de Lafuente, V. & Romo, R. Neural correlate of subjective sensory experience gradually builds up across cortical areas. *Proc. Natl. Acad. Sci. USA* **103**, 14266–14271 (2006).
50. Dehaene, S. & Changeux, J.P. Experimental and theoretical approaches to conscious processing. *Neuron* **70**, 200–227 (2011).

ONLINE METHODS

All experimental procedures were approved by the Swiss Federal Veterinary Office.

Training mice to report whisker deflection. Male C57BL/6J mice, GAD67-GFP mice[51], Emx1-Cre mice[52], GAD2-Cre mice[53] and PV-Cre mice[54] crossed to lox-stop-lox tdTomato[55] reporter mice were implanted with a metal head-restraint post at 4–9 weeks after birth under isoflurane anesthesia. All whiskers were trimmed except for the C2 whiskers on either side. Intrinsic signal optical imaging was carried out to locate the C2 barrel column in the left hemisphere[56]. Over a period of a few days, the mice were adapted to the head restraint. During subsequent behavioral training days, the mice were water restricted, receiving their water in the behavioral setup and having brief access to wet food immediately after each training session. Iron filings were applied to the right C2 whisker at the beginning of each training session, allowing the right C2 whisker to be vertically deflected with a brief magnetic pulse 1 ms in duration. Mice were taught to associate whisker deflection with water availability. If they licked the reward spout within the reward time window, it was considered a hit trial, and they obtained a drop of water. If they did not lick within the reward window, it was considered a miss trial, and no reward was delivered. The reward window differed for different mice, ranging from the shortest reward window of 0–500 ms after whisker stimulus to the longest reward window of 0–1,000 ms after whisker stimulus. Whisker stimuli were delivered without preceding cues at random interstimulus intervals ranging from 2–8 s. If the mouse licked in the 2 s preceding the time when the whisker stimulation was supposed to occur, then the trial was aborted. In otherwise identical trials, the whisker was not stimulated (catch trials) to test for licking unrelated to the magnetic whisker stimulus. Catch trials were randomly interleaved with whisker stimulus trials, and if the animal licked during a catch trial (false alarm), no reward was delivered. When the mouse did not lick during a catch trial, it was considered as a correct rejection, which was not rewarded. Catch trials were introduced starting on day 2 of training. Mice were able to learn the detection task rapidly and displayed a stable level of performance after a few days of training with a low false-alarm rate. Ambient white noise was played at all times to mask any potential auditory cues. Licks were detected with piezo film attached to the reward spout. In some experiments, whisker movement was filmed with a high-speed (500 Hz) camera (MotionPro, Redlake) under infrared illumination. Behavioral control and behavioral data collection were carried out with custom-written computer routines using either an ITC18 (Instrutech) interfaced through IgorPro (Wavemetrics) or a National Instruments board interfaced through LabView. Once the mice achieved a consistent hit rate above 80% and false alarms at lower than 30%, they were considered well trained and were subsequently used in pharmacological inactivation, optogenetic (in)activation or electrophysiological recording experiments.

Pharmacological inactivation. Under isoflurane anesthesia, a small craniotomy was performed over the C2 barrel column (or, in a few control experiments, the forepaw representation) in the primary somatosensory cortex of the left hemisphere as identified by intrinsic signal optical imaging. The mouse was allowed to recover from anesthesia in its home cage. Subsequently, the mouse was taken to the experimental setup, and behavioral performance in the detection task was assessed. In highly performing mice, injections of 100 nl were carried out during the detection task at 1,000, 800, 600, 400 and 200 µm depths below the pial surface using a hydraulic injection system (Narishige) with a glass micropipette attached to a micromanipulator. To block action potentials, TTX was injected at a micropipette concentration of 10 µM dissolved in Ringer's solution containing (in mM) 135 NaCl, 5 KCl, 5 4-(2-hydroxyethyl)-1-piperazineethanesulfonic acid (HEPES), 1.8 $CaCl_2$, 1 $MgCl_2$. Ionotropic glutamatergic synaptic transmission was blocked by injecting a mixed cocktail of 200 µM CNQX and 500 µM AP5. LFPs were recorded in layer 2/3 of the C2 barrel column before and after injections to verify pharmacological inactivation. Recovery was quantified ~30 min after injection of CNQX and AP5. Recovery was quantified on the day after injection of TTX.

Optogenetic activation. Emx1-Cre mice (6–9 weeks old, both male and female) (B6.Cg-Emx1tm1 (Cre) Krj/J; Cre recombinase expressed from the endogeneous Emx-1 locus) (JAX stock number 005628)[52] were injected under isoflurane anesthesia with an adeno-associated virus serotype 5 expressing a double-floxed inverted open reading frame of humanized ChR2 (His134 converted to arginine) fused to enhanced YFP (eYFP) under the control of the EF1α promoter (AAV2/5 DIO-EF1α-hChR2^{H134R}-eYFP; virus made by Penn Vector Core)[21]. Before virus injection, a 3 mm craniotomy was made on the left hemisphere over the C2 barrel column located using intrinsic signal optical imaging. The dura was left intact. An injection micropipette (internal tip diameter, ~20 µm) was tip filled with the virus solution and lowered into the C2 barrel column. Injections of ~350 nl were carried out at depths of ~700 and ~300 µm below the pia to infect cells in layers 2–5. The micropipette was allowed to remain in the brain for 5 min before being retracted slowly over a period of 8–10 min to prevent backflow of the virus along the shaft. To make a cranial window, a circular coverslip (4 mm in diameter) was placed over the craniotomy, and the edges were sealed with cyanoacrylate glue and dental cement[22,57]. The condition of the cranial window and the brightness of fluorescence were assessed after allowing 3–4 weeks for expression. In mice in which ChR2 was expressed in the S1-forepaw representation, the latter was located with intrinsic optical imaging, and the virus was injected as described above.

Mice expressing ChR2 were trained in the whisker detection task following identical protocols as those described above for uninjected mice, except that they were trained in an environment with ambient blue light. On the transfer test day, a third kind of trial (ChR2 stimulus trial) was randomly interleaved with the whisker stimulus and catch trials. The light stimulus consisted of a single pulse of blue light with a duration of 1, 3, 5 or 10 ms. Light stimuli were delivered to the barrel cortex by a multimode fiber-optic cable (Thorlabs; numerical aperture (NA) 0.37, 400 µm) coupled to a 473-nm blue light-emitting diode (LED) (Luxeon Rebel). The outer cladding of one end of the cable was stripped, and this end was glued to the LED and reinforced with epoxy and dental cement. The other end of the fiber was also stripped, and this end was mounted on a micromanipulator that was lowered until the tip of the optical fiber touched the cranial window.

Other mice were trained to lick in response to optogenetic activation of S1 barrel cortex. Training procedures were identical to those used for the mice learning the whisker stimulus detection task, except the whisker stimuli were replaced by blue light flashes delivered to the barrel cortex, and training was carried out with ambient blue light. As with the whisker task, for the optogenetic task, we quantified hit, miss, false-alarm and correction-rejection outcomes. The training stimulus always consisted of a single light pulse of 5 ms. On the transfer test day, mice that displayed stable hit rates (80%) with low false alarms (30%) in response to optogenetic stimuli were challenged with magnetic whisker stimuli randomly interleaved with optogenetic stimulus trials and catch trials. At end of the experiment, mice were anesthetized and perfused, and their brains were recovered for histology to verify the injection sites.

Optogenetic inactivation. PV-Cre mice[54] crossed to lox-stop-lox tdTomato[55] reporter mice (5-week-old males) were injected with the same AAV2/5 DIO-EF1α-hChR2^{H134R}-eYFP vector as described above in the C2 barrel column, which was identified through intrinsic signal optical imaging. A single injection of ~350 nl was carried out at a depth of ~300 µm below the pia through a ~0.5 mm craniotomy.

Mice expressing ChR2 in PV neurons were trained in the whisker stimulus detection task, as described above, in an environment with ambient blue light. On the day of optogenetic S1 inactivation, a third kind of trial (ChR2 stimulus trial coupled with whisker stimulus) was randomly interleaved with the whisker stimulus and catch trials. The light stimulus consisted of a 200 Hz train of blue light pulses, each with a duration of 3 ms. To block the early sensory response, the blue light train was applied 1 ms before the onset of whisker stimulus for a duration of 60 ms. To block the secondary late response, the blue light train was applied 100 ms after the whisker stimulus for a duration of 155 ms. Light stimuli were delivered to the barrel cortex by a 473-nm blue LED (Luxeon, Philips) focused through a 40× 0.9 NA objective (Olympus). At the end of the experiment, mice were anesthetized and perfused, and their brains were recovered for histology to verify the injection sites.

Facial nerve transection. Animals were anesthetized with ketamine and xylazine, and an incision was made in the skin covering the right cheek to expose the extraorbital gland. At the level of the extraorbital gland, the *ramus temporalis*, *ramus zygomatico-orbitalis* and *ramus buccolabialis-superior* were transected.

doi:10.1038/nn.3532

Rostral to this, the dorsal branch of the *buccolabialis-inferior* was transected, thus cutting off inputs to both intrinsic and extrinsic muscles[58]. The skin was sutured back. Betadine and a topical antibiotic (Cicatrex) were applied over the skin. The efficacy of the nerve cut was confirmed by the lack of rhythmic whisking on the right side, whereas whisking on the left side appeared unaffected.

Whole-cell, local field potential and juxtasomal recordings. Recording electrodes were targeted to the C2 barrel column identified through intrinsic signal optical imaging[10,11,24,26,28,29]. All recordings were obtained from layer 2/3 using standard glass patch-clamp electrodes with a resistance of ~5 MΩ. Typically, two recording electrodes (for example, one whole-cell recording electrode together with one LFP electrode or two juxtasomal recording electrodes) were simultaneously advanced to the same subpial depth, with the electrode tips within ~200 µm of each other. The whole-cell pipette solution contained (in mM): 135 potassium gluconate, 4 KCl, 10 HEPES, 10 sodium phosphocreatine, 4 MgATP, 0.3 Na_3GTP (adjusted to pH 7.3 with KOH) and 2 mg ml^{-1} biocytin. Extracellular electrodes for recording LFP or juxtasomal spiking were filled with Ringer's solution containing (in mM): 135 NaCl, 5 KCl, 5 HEPES, 1.8 $CaCl_2$ and 1 $MgCl_2$. Most experiments were carried out in C57BL/6J mice, but GAD67-GFP mice[51] and GAD2-Cre mice[53] crossed to lox-stop-lox tdTomato[55] reporter mice were used to visualize GABAergic neurons, and PV-Cre mice[54] crossed to lox-stop-lox tdTomato[55] reporter mice were used to visualize fast-spiking PV-expressing GABAergic neurons in some recordings carried out under visual control with a custom-built two-photon microscope[11,28,29,59,60]. For the two-photon targeted recordings, 10 µM Alexa-594 (for recording GFP neurons) or Alexa-497 (for recording PV-tdTomato neurons and unlabeled excitatory neurons in GAD2-tdTomato mice) was added to the pipette solution. A pulsed laser (MaiTai HP) focused 880-nm or 920-nm light into the cortex using a 40× 0.9 NA objective (Olympus), and fluorescence was detected on red and green channels (red, 607 ± 35 nm (range); green, 510 ± 42 nm) using photomultiplier tubes (Hamamatsu). All electrophysiological measurements were made with a Multiclamp 700B amplifier (Molecular Devices). V_m was not corrected for the liquid junction potential. V_m was filtered at 10 kHz and digitized at 20 kHz by an ITC-18 under the control of IgorPro. FFTs were computed as magnitudes in IgorPro for 2-s segments of the recordings immediately before the whisker stimulus. The amplitude of low-frequency V_m fluctuations was calculated by integrating the computed FFTs from 1 to 5 Hz. Cross correlations of V_m changes were computed by subtracting the average value of each trace, normalizing each trace to its s.d. and then computing the correlation in IgorPro to generate a cross correlogram with a maximal value of 1 for identical traces.

Statistical analyses. All values are presented as the mean ± s.e.m. Statistical testing was carried out in IgorPro and Microsoft Excel. The Anderson-Darling test was done on all the data to test for normality. We used Student's two-tailed paired or unpaired *t* test for parametric data and the Wilcoxon signed-rank paired test and Wilcoxon-Mann-Whitney test for paired and unpaired nonparametric data, and all tests were two sided. No blinding or randomization was done. Tests to determine sample size were not performed, and our sample sizes were similar to those used in previous publications in the field[7,28,29].

51. Tamamaki, N. *et al.* Green fluorescent protein expression and colocalization with calretinin, parvalbumin, and somatostatin in the GAD67-GFP knock-in mouse. *J. Comp. Neurol.* **467**, 60–79 (2003).
52. Gorski, J.A. *et al.* Cortical excitatory neurons and glia, but not GABAergic neurons, are produced in the Emx1-expressing lineage. *J. Neurosci.* **22**, 6309–6314 (2002).
53. Taniguchi, H. *et al.* A resource of Cre driver lines for genetic targeting of GABAergic neurons in cerebral cortex. *Neuron* **71**, 995–1013 (2011); erratum **72**, 1091 (2011).
54. Hippenmeyer, S. *et al.* A developmental switch in the response of DRG neurons to ETS transcription factor signaling. *PLoS Biol.* **3**, e159 (2005).
55. Madisen, L. *et al.* A robust and high-throughput Cre reporting and characterization system for the whole mouse brain. *Nat. Neurosci.* **13**, 133–140 (2010).
56. Ferezou, I., Bolea, S. & Petersen, C.C.H. Visualizing the cortical representation of whisker touch: voltage-sensitive dye imaging in freely moving mice. *Neuron* **50**, 617–629 (2006).
57. Holtmaat, A. *et al.* Long-term, high-resolution imaging in the mouse neocortex through a chronic cranial window. *Nat. Protoc.* **4**, 1128–1144 (2009).
58. Dörfl, J. The musculature of the mystacial vibrissae of the white mouse. *J. Anat.* **135**, 147–154 (1982).
59. Margrie, T.W. *et al.* Targeted whole-cell recordings in the mammalian brain *in vivo*. *Neuron* **39**, 911–918 (2003).
60. Kitamura, K., Judkewitz, B., Kano, M., Denk, W. & Häusser, M. Targeted patch-clamp recordings and single-cell electroporation of unlabeled neurons *in vivo*. *Nat. Methods* **5**, 61–67 (2008).